

Principal Component Analysis for the Study of Opening Underground Caverns in Salt Rocks

Rayra Amorim^{a*}, Leonardo Guimarães^b, Oscar Melgar^c

^{a,b,c}Dept. of Civil Engineering, Federal University of Pernambuco, Av. Prof. Moraes Rego, 1235, Cidade Universitária, Recife, 50670-901, Pernambuco, Brazil

^aEmail: rayra.amorimsilva@ufpe.br

^bEmail: leonardo.guimares@ufpe.br

^cEmail: oscar.melgar@ufpe.br

Abstract

The constant dynamism within the oil industry associated with the need for new technologies in terms of production and disposal of products were fundamental for the increase of studies about the use of underground caverns in salt rocks as an alternative for the storage of petroleum products. Salt rock is particularly useful for storage because of its low cost, low permeability, and its healing potential when compared to other rocks, including granite, mud, and basalt. The opening process and subsequent development of these cavities are complex activities and the variables involved in the process play a crucial role during the entire operation. In this sense, the present work aims to identify, through the PCA (Principal Component Analysis) statistical tool, the variables that most influence the process of opening a salt cavern by dissolution. For this, numerical simulations of the dissolution mining process for opening a cavern under typical conditions of water injection into a salt rock using the software SALGAS were developed considering different methods of saline water circulation, after that, the variables injection temperature, injection rate, radius, volume, pump power, cumulative energy, tubing loss, produced brine, pump pressure, injection pressure, and salt dissolution factor were interpreted using the multivariate statistical tool through software PAST. For the simulations generated, the results with the statistical tool were satisfactory, it was found that the brine injection rate contributes significantly to the process, in terms of x-axis, directly influencing the behavior of other variables, the temperature have a great importance to the y-axis. Regarding the total variability of the data, more than 97% of these could be represented in terms of the first two components for both scenarios studied.

Keywords: cavern; salt rock; process variables; numerical simulations; statistical analysis.

* Corresponding author.

1. Introduction

The growing global energy demand requires the search for new techniques for the safe storage of products.

In this sense, salt rock is considered the ideal material for underground storage due to low permeability, healing capacity, and availability [1]. In addition, underground salt caverns can be built by solution mining techniques, which are cheaper than other conventional excavation techniques [2]. When compared to other rocks, including granite, mud, and basalt the cost of leaching caverns by dissolution in salt rock turns out to be lower. Another advantage is the ability to absorb harmful nuclear radiation (in a waste storage medium and water solubility, an ideal choice for the deep burial of nuclear waste and oil and gas storage) [3].

The dissolution of the salt rock contemplates the initial phase of opening of these cavities, being one of the first experimental studies on the subject, that of Durie & Jessen [4] who carried out a series of laboratory tests in order to evaluate the influence of the injection rate of water (fresh and salty) in the cavern formation rate and the salt removal rate. The injection rate of water was one of the main parameters in our study, being important to know works that approach the behavior of this and other variables. In addition to experimental studies, mathematical and numerical modeling were also developed in this field.

Also, in the work of Durie & Jessen [4], a mathematical model was presented that describes the dissolution process as a function of the salinity of the water at any point on the vertical surface of the salt. It was found that at low injection rates, the induced flow does not significantly contribute to the salt removal rate, which means that it is the high injection rates that really influence the process. Saberian [5] developed a 5" tall cylindrical model to study the flow and expansion mechanisms of saline cavities during dissolution, the results combined into a generalized numerical model, where the prediction of cavity dissolution as a function of the time and also other physical parameters such as velocity, radius, and dissolution rate. These other parameters besides injection rate of water were also important in our study. More recently Yang et al. [6] presented a proposal for an analytical solution of a differential equation to calculate the dissolution rate of saline rocks subjected to an instantaneous diffusion process, the results showed a fit between the numerical model and the experiment of the salt concentration with concerning to time.

As these are numerical aspects, the parameters involved in numerical simulations can also be interpreted from a statistical perspective. Multivariate data analysis can reduce data or carry out a structural simplification as well as investigate the dependency relationship between variables [7]. This set of statistical methods is widely used in various fields of science and encompasses different techniques, the most used being cluster analysis, factor analysis, principal component analysis, multiple regression, and logistic regression, each with its characteristics.

In the present work, a finite difference code, SALGAS is used to predict response surfaces for these caverns, this method solves differential equations based on the finite difference derivative approximation. After the surface generation, the numerical data analysis was performed with the PCA (Principal Component Analysis) statistical tool through the software PAST. In this method, an orthogonal transformation is performed to convert a set of observations of possibly correlated variables into a set of values of linearly uncorrelated variables called Principal

Components (PC) that reveal the internal structure of the data in a way that best explains its variance [8].

In this context, this work aims to investigate the degree of influence that each variable has individually on the process of opening an underground cavern in salt rock.

2. Materials and methods

Two hypothetical scenarios were considered for the study of the opening of an underground cavern in salt rock by dissolution, scenario D where water was injected at the bottom of the cavern and the brine was extracted from the top of it, through the so-called direct circulation method, and the scenario R where water was injected at the top of the cavern and the brine was extracted from the bottom of the cavern, in the so-called reverse circulation method. In Table 1 the respective injection and production heights are presented for the considered scenarios and in Figure 1 their schematic representation.

Table 1: Injection and Production depths for the proposed hypothetical scenarios

SCENARIO	ID (ft)	ID (m)	PD (ft)	PD(m)
SCENARIO D	3000	914.4	2500	762
SCENARIO R	2500	762	3000	914.4

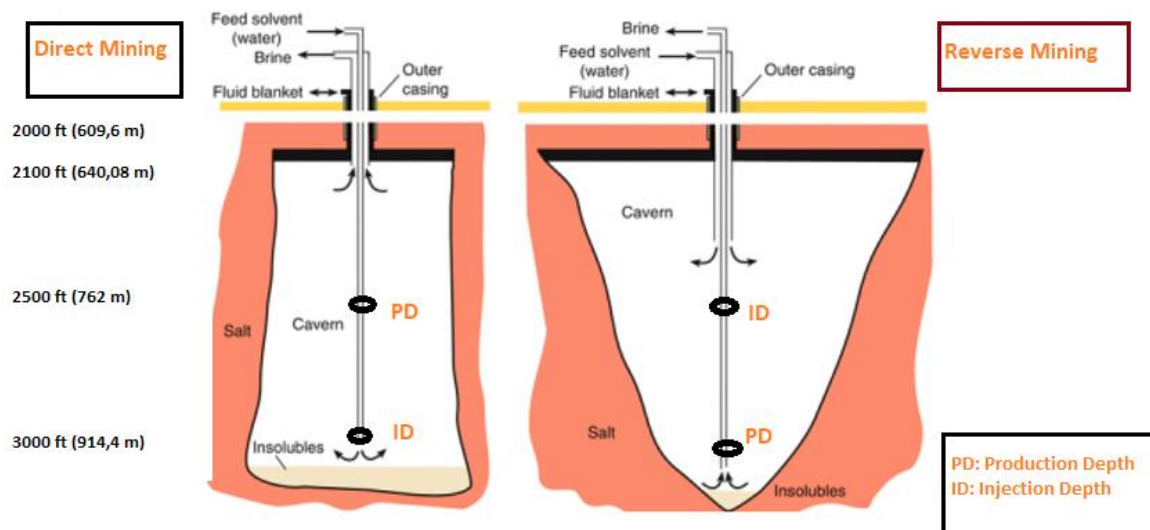


Figure 1: Scenarios of salt cavern opening by dissolution. Source: Adapted from [9]

For the numerical modeling of the approached scenarios was used the SALGAS software, written in FORTRAN in the mid-1970s. This finite difference code developed by the Solution Mining Research Institute (SMRI) to simulate the dissolution of sodium chloride salt by water, optionally simulates the hydraulic properties and power requirements of the mining system. The main limitation of this software is the impossibility to simulate offshore scenarios, which limits the reach of the proposed scenarios.

Both scenarios were based on example number 1 from the SALGAS Manual [10]. In this example, the

development of a new cavern is started from a hole with a blanket, which moves up once, with 3% insolubles, considering a constant brine injection rate and equal to 750 gpm (170.34 m³/h) and the SALGAS base temperature of 75°F (23.9°C) during 120 days. The hydraulic model has a short section of surface piping and divides each of the piping lines into two sections.

From this base situation, new simulations were obtained in this study by varying the injection temperature and the brine injection rate. The injection pressure, P (MPa) is the difference between the pressure of the fluid to be injected, P₁ (MPa) and the pressure of fluid in the massive, P₂ (MPa). With P₂ known, the Bernoulli equation, only valid for incompressible fluids, is used to find P₁, through Equation 1:

$$\frac{P_1}{\gamma} + \frac{v_1^2}{2g} + z_1 = \frac{P_2}{\gamma} + \frac{v_2^2}{2g} + z_2 \quad (1)$$

Where: g = gravity acceleration (m/s²); P = pressure (Pa); v = velocity (m/s); z = height (m); γ = specific weight (N/m³), and z; v = flow/area; γ = ρg. The initial brine specific gravity and the injection fluid specific gravity are input parameters for SalGas obtained from the Toolbox provided by SMRI. The brine pressure and temperature values are entered and the Toolbox automatically provides the parameters, to determine the brine produced, it is also necessary to inform the fluid saturation which is 4.05% in NaCl.

According to Saberian [11], it is possible to obtain the dissolution rate of a brine, m_T (cc/cm²/min x 10³), for different temperatures and salinities, as a function of the specific density of the brine, ρ (-), of the reference temperature, T₀ (°F), and the initial production temperature, T (°F), according to Equation 2:

$$m_T = 0.22(1.2019 - \rho)^{1.42} \exp \left[0.0119 \left(\frac{\rho - 1}{1.2019 - \rho} \right)^{0.2} \Delta T \right] \quad (2)$$

As in SalGas the reference temperature is 75°F and all the simulations performed are isothermal fixed for this temperature, the input data instead of being the dissolution rate is the dissolution factor which is the exponential term of Equation 2 for an ideal salt (T₀=75°F and ρ=1.20). The dissolution factor, DF corrects the dissolution rate by compensating between a 75°F isothermal simulation of an “ideal salt”, which would generate a brine with the maximum specific gravity accepted by the software = 1.2, and the simulation that needs to be done, with temperature and specific densities different from the ideal. DF is given by Equation 3:

$$DF = \exp \left[0.0119 \left(\frac{\rho - 1}{1.2019 - \rho} \right)^{0.2} \Delta T \right] \quad (3)$$

The diameters of the external and internal piping were the same as those considered in the example, respectively 10¾” (273.05 mm) and 7” (177.8 mm). The mining module of SALGAS was used together with the hydraulic module to simulate the dissolution of the rock.

Tables 2 and 3 present the parameters that were used in the SALGAS data input file for scenarios D and R respectively.

Table 2: Input parameters for Scenario D

N	Injection Temperature (°C)	Injection Rate (m ³ /h)	Injection Pressure (MPa)	Initial Brine Density	Injected Fluid Density	Salt Dissolution Factor
1	40	120	9.0500	1.196300	1.023930	1.25989419
2	40	200	9.1800	1.196400	1.024030	1.26016984
3	40	360	9.6700	1.196500	1.024230	1.26071911
4	40	400	9.8300	1.196600	1.024330	1.26099276
5	40	800	12.4200	1.197600	1.025430	1.26396075
6	40	1200	16.7400	1.199400	1.027130	1.26840665
7	60	120	9.0500	1.187400	1.014330	1.58798018
8	60	200	9.1800	1.187400	1.014530	1.59017741
9	60	360	9.6700	1.187600	1.014630	1.59126914
10	60	400	9.8300	1.187600	1.014730	1.59235636
11	60	800	12.4200	1.188700	1.015830	1.60403307
12	60	1200	16.7400	1.190500	1.017630	1.62214403
13	80	120	9.0500	1.179100	1.002830	1.67090079
14	80	200	9.1800	1.179100	1.002930	1.67697674
15	80	360	9.6700	1.179300	1.003130	1.68871982
16	80	400	9.8300	1.179400	1.003230	1.69440201
17	80	800	12.4200	1.180400	1.004330	1.75029718
18	80	1200	16.7400	1.182300	1.006130	1.82428703

Table 3: Input parameters for Scenario R

N°	Injection Temperature (°C)	Injection Rate (m ³ /h)	Injection Pressure (MPa)	Initial Brine Density	Injected Fluid Density	Salt Dissolution Factor
1	40	120	7.5600	1.195700	1.023330	1.25822596
2	40	200	7.7100	1.195800	1.023430	1.25850574
3	40	360	8.2300	1.196000	1.023530	1.25878481
4	40	400	8.4100	1.196000	1.023630	1.25906319
5	40	800	11.2200	1.197200	1.024830	1.26235126
6	40	1200	15.9000	1.199000	1.026730	1.26737505
7	60	120	7.5600	1.186800	1.013730	1.58127404
8	60	200	7.7100	1.186800	1.013830	1.58240401
9	60	360	8.2300	1.187000	1.014030	1.58464903
10	60	400	8.4100	1.187100	1.014130	1.58576420
11	60	800	11.2200	1.188200	1.015330	1.59878792
12	60	1200	15.9000	1.190100	1.017230	1.61821655
13	80	120	7.5600	1.178500	1.002230	1.63097469
14	80	200	7.7100	1.178500	1.002330	1.63810134
15	80	360	8.2300	1.178700	1.002530	1.65174855
16	80	400	8.4100	1.178800	1.002630	1.65829672
17	80	800	11.2200	1.179900	1.003830	1.72622905
18	80	1200	15.9000	1.181900	1.005730	1.80920606

After running the cases in SALGAS, the production variables in addition to the volume and radius of the cave in the proposed final time (120 days) had their data selected together with the input variables injection temperature, brine injection rate, injection pressure, and salt dissolution factor to be statistically analyzed by the PAST software, through the technique of PCA.

Table 4: Input parameters for the PAST software: Scenario D

Injection Temperature (°C)	Injection Rate (m³/h)	Radius (m)	Volume (m³)	Pump Power (kW)	Cumulative Energy (J)	Tubing Loss (MPa)	Produced Brine (m³)	Pump Pressure (MPa)	Injection Pressure (MPa)	Salt Dissolution Factor
40	120	7.7694	37213.41616	658.4531	6.6829E+11	0.1502	334211.3423	1.7878	9.0500	1.25989419
40	200	9.4031	57141.62737	1429.5069	1.45308E+12	0.3816	557057.8557	2.3318	9.1800	1.26016984
40	360	11.8049	92203.71572	4639.7454	4.73274E+12	1.1280	1002038.7796	4.2044	9.6700	1.26071911
40	400	12.2682	99816.80821	5941.7376	6.06455E+12	1.3755	1109596.3469	4.8381	9.8300	1.26099276
40	800	15.8313	166230.4175	34571.3977	3.56105E+13	4.9684	2230660.5850	14.1687	12.4200	1.26396075
40	1200	17.9192	212801.6161	103292.8726	1.08158E+14	10.4662	3329176.0150	28.5650	16.7400	1.26840665
60	120	8.3972	41667.42743	709.9064	7.21642E+11	0.1507	334211.3423	1.9154	9.0500	1.58798018
60	200	10.0614	64858.28877	1518.9909	1.54811E+12	0.3818	557057.8557	2.4656	9.1800	1.59017741
60	360	12.7224	106726.4532	4892.5377	4.96045E+12	1.1425	1002038.7796	4.3844	9.6700	1.59126914
60	400	13.2466	116042.2662	6068.5066	6.2317E+12	1.3617	1109596.3469	4.9463	9.8300	1.59235636
60	800	17.4315	201898.7646	35147.0781	3.62468E+13	4.9725	2230660.5850	14.3342	12.4200	1.60403307
60	1200	20.0497	265475.1015	104578.4594	1.09958E+14	10.4731	3329176.0150	28.7718	16.7400	1.62214403
80	120	8.7325	44843.31677	750.9199	7.6468E+11	0.1501	334211.3423	2.0209	9.0500	1.67090079
80	200	10.4760	70250.0149	1599.5265	1.62383E+12	0.3832	557057.8557	2.5786	9.1800	1.67697674
80	360	13.2801	116354.5469	4988.733	5.07783E+12	1.1321	1002038.7796	4.4685	9.6700	1.68871982
80	400	13.8440	126798.4618	6128.9083	6.34018E+12	1.3383	1109596.3469	5.0077	9.8300	1.69440201
80	800	18.4038	225757.1488	36343.9266	3.67627E+13	5.0421	2230660.5850	14.6307	12.4200	1.75029718
80	1200	21.4213	305255.9144	108662.6583	1.1227E+14	10.6800	3329176.0150	29.4406	16.7400	1.82428703

Table 5: Input parameters for the PAST software: Scenario R

Injection Temperature (°C)	Injection Rate (m³/h)	Radius (m)	Volume (m³)	Pump Power (kW)	Cumulative Energy (J)	Tubing Loss (MPa)	Produced Brine (m³)	Pump Pressure (MPa)	Injection Pressure (MPa)	Salt Dissolution Factor (DF)
40	120	9.7384	41584.35672	624.1509	6.38849E+11	0.1605	334211.3423	1.6885	7.5600	1.25822596
40	200	11.7653	64401.4905	1395.9504	1.42797E+12	0.4075	557057.8557	2.2698	7.7100	1.25850574
40	360	14.5786	104419.1241	4654.6594	4.77441E+12	1.1997	1002038.78	4.2106	8.2300	1.25878481
40	400	15.0967	113043.1148	5985.7339	6.12315E+12	1.4576	1109596.347	4.8629	8.4100	1.25906319
40	800	19.0378	189170.0651	34992.7182	3.67585E+13	5.2835	2230660.585	14.2997	11.2200	1.26235126
40	1200	21.3787	244061.1218	107118.3136	1.1174E+14	11.3074	3329176.015	29.5027	15.9000	1.26737505
60	120	10.4638	45842.4658	659.9445	6.78539E+11	0.1609	334211.3423	1.7802	7.5600	1.58127404
60	200	12.7467	72203.79183	1457.0978	1.49936E+12	0.4087	557057.8557	2.3670	7.7100	1.58240401
60	360	15.9258	119336.2686	4803.7994	4.92558E+12	1.2045	1002038.78	4.3265	8.2300	1.58464903
60	400	16.5384	129867.4276	6131.8911	6.29215E+12	1.4638	1109596.347	4.9718	8.4100	1.58576420
60	800	21.1988	225099.0809	35408.0731	3.69047E+13	5.3159	2230660.585	14.5204	11.2200	1.59878792
60	1200	24.2286	300251.0434	110101.8593	1.13889E+14	11.3901	3329176.015	29.9646	15.9000	1.61821655
80	120	10.8692	48891.77127	693.501	7.13102E+11	0.1609	334211.3423	1.8643	7.5600	1.63097469
80	200	13.2862	77437.07788	1517.4995	1.55969E+12	0.4087	557057.8557	2.4518	7.7100	1.63810134
80	360	16.6634	128735.2716	4864.9468	5.02142E+12	1.2045	1002038.78	4.3906	8.2300	1.65174855
80	400	17.3401	140390.4591	6262.3886	6.42679E+12	1.4638	1109596.347	5.0566	8.4100	1.65829672
80	800	22.4516	248085.5009	35762.2806	3.71783E+13	5.3221	2230660.585	14.6031	11.2200	1.72622905
80	1200	26.0634	339761.6182	110544.8051	1.14688E+14	11.4108	3329176.015	30.0060	15.9000	1.80920606

3. Results and discussions

3.1. Results with SALGAS

Based on the simulations performed in the SALGAS software, it was possible to compare the D and R scenarios, through curves. The behavior of the cavern was analyzed considering the variation of the injection temperature and the brine injection rate along time of 120 days. Figures 2 and 3 bring the main simulations for scenario D.

The comparison of the final contour of the cavern for the time of 120 days considering all analyzed cases was presented in figure 2, where it was possible to verify the geometry and the value of the radius reached. The maximum value reached for the time of 120 days was approximately 22 m of radius for the temperature of 80°C and injection rate of 1200 m³/h. Analyzing the same rate value, the cavern radius increases with increasing temperature, but this seems to have less influence on the final diameter obtained than the rate.

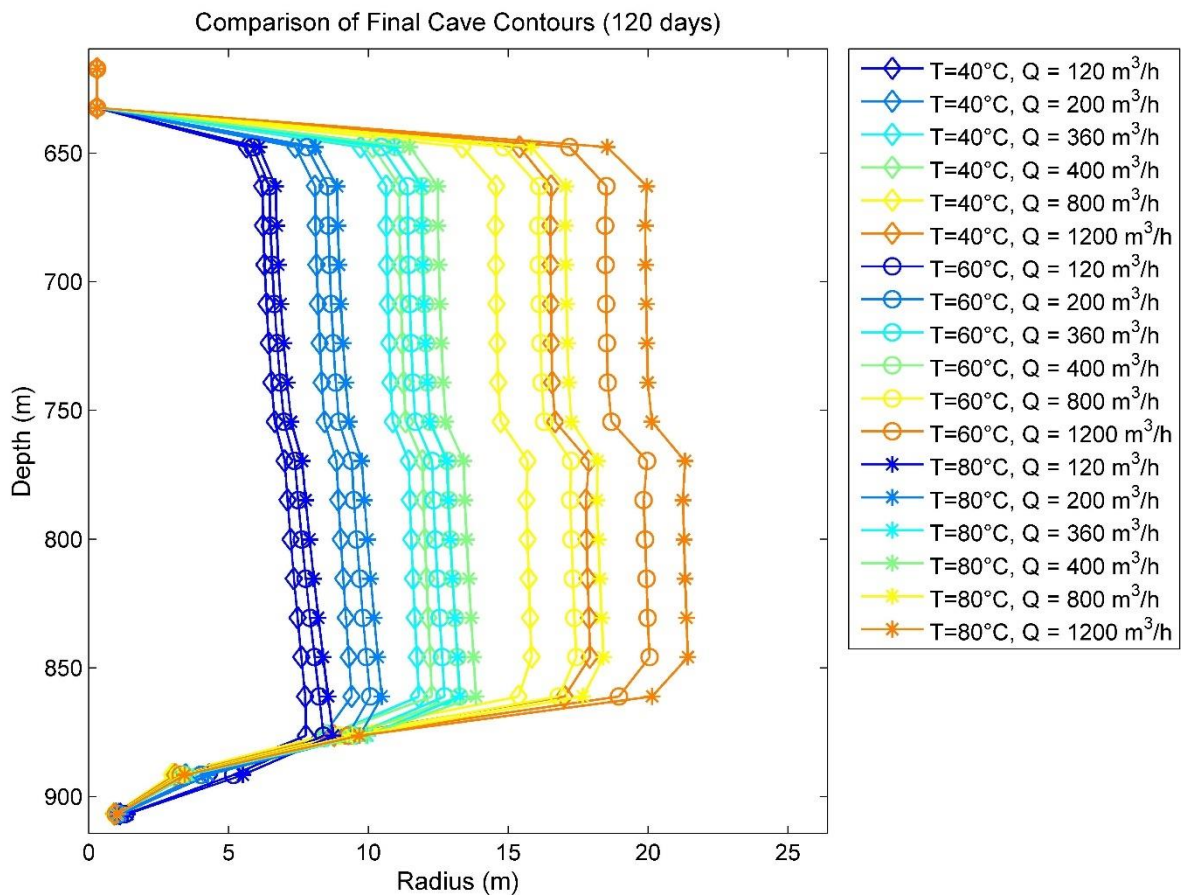


Figure 2: Comparison of final cavern contours: all simulations

In addition to the cavern geometry, the evolution of its volume was evaluated. For the same temperature, the volume grows faster for higher rates. Figure 3 shows all cases analyzed (all rates and temperatures). Analyzing the influence of temperature, it is observed that for the same rate, the higher the temperature, the greater the volume of the cavern.

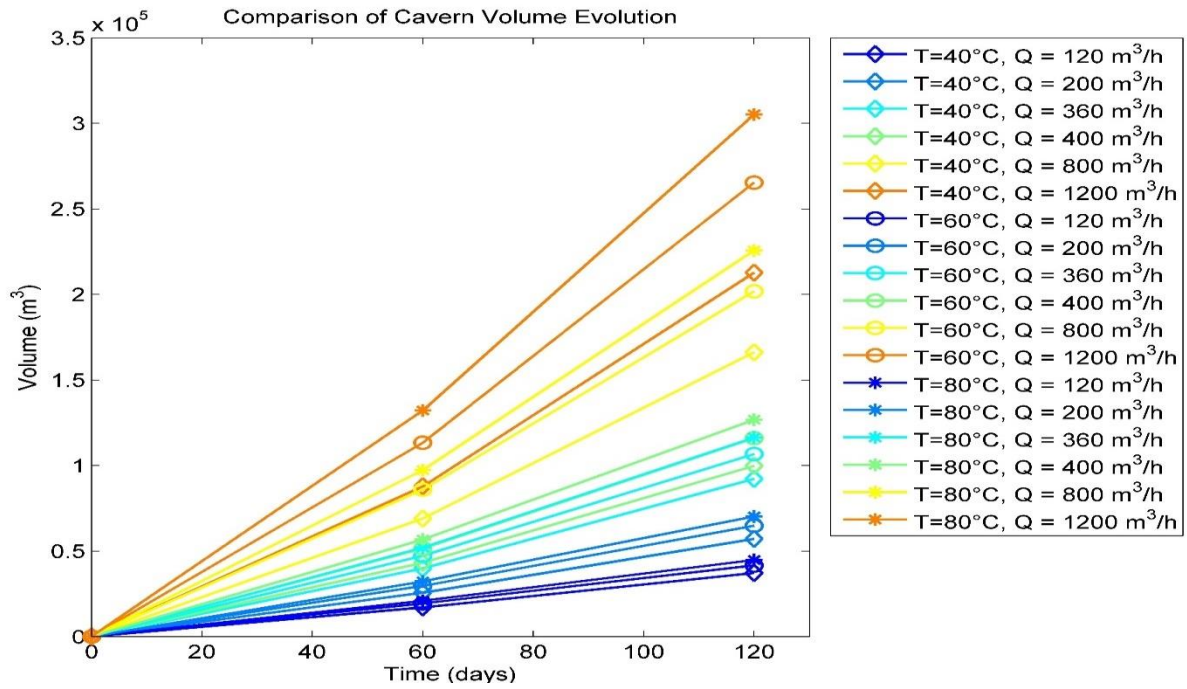


Figure 3: Comparison of final cavern volume evolution: all simulations

Figures 4 and 5 bring the main simulations for scenario R. Similar to what happens in scenario D, for the same temperature, the higher the injection rate, the greater the radius of the cavern. The maximum value reached for the time of 120 days was approximately 26 m of radius for the temperature of 80°C and injection rate of 1200 m³/h (Figure 4).

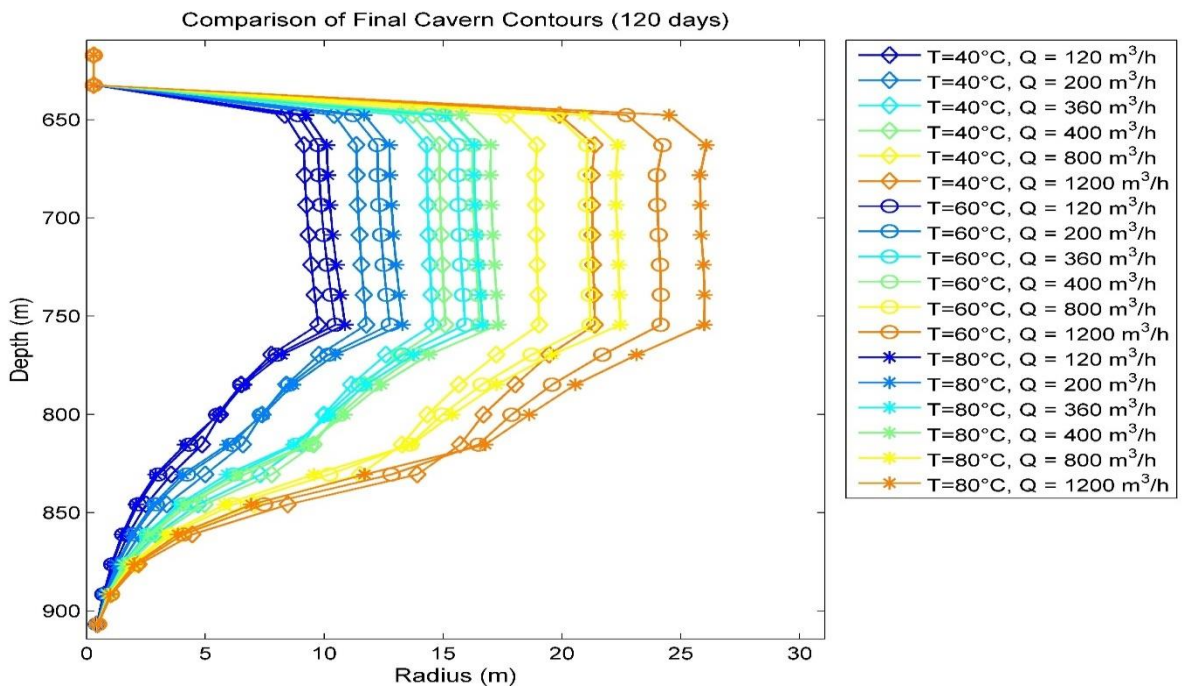


Figure 4: Comparison of final cavern contours: all simulations

Figure 5 shows the evolution of the cavern volume for all cases analyzed (all rates and temperatures). Analyzing the influence of temperature, it is observed that for the same rate, the higher the temperature, the greater the volume of the cavern.

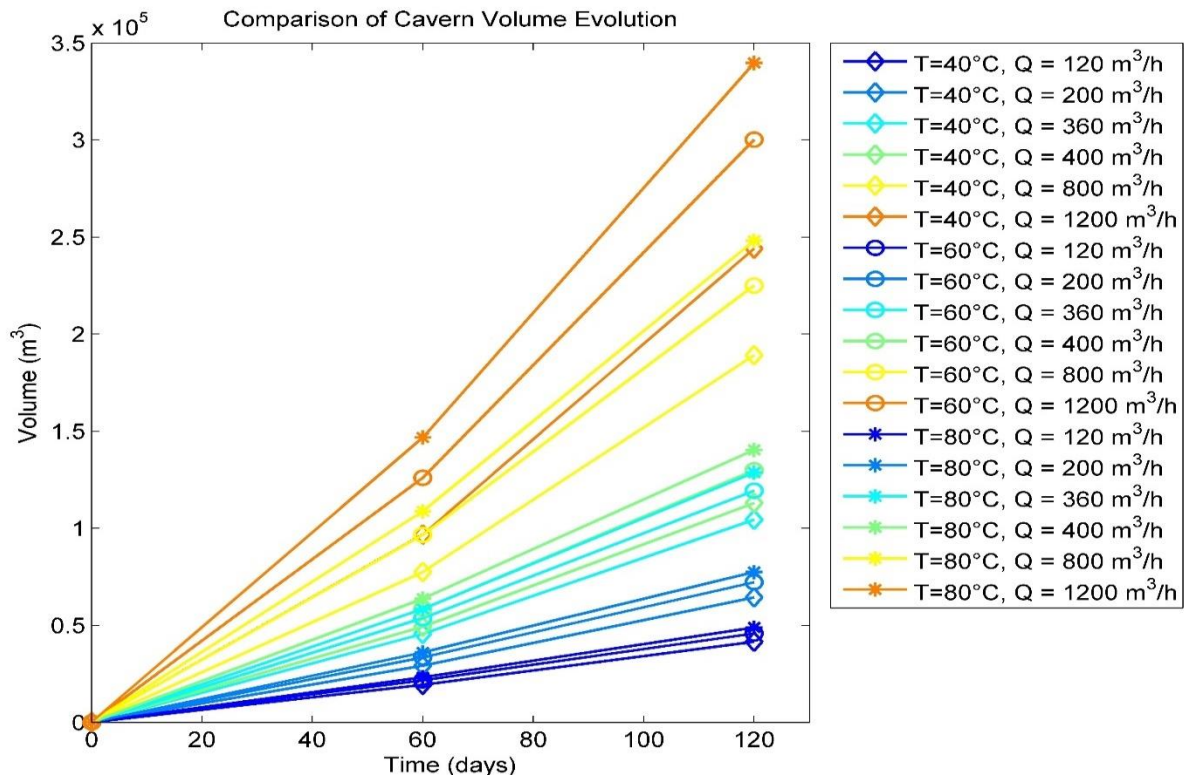


Figure 5: Comparison of final cavern volume evolution: all simulations

3.2 Results with PCA

For each of the scenarios studied, statistical analysis of the data was performed considering the principal components technique. The main results are presented below.

For scenario D, Table 6 presents the respective eigenvalues and the percentages of variance explained by each one. In the study with 11 parameters of simulations for the opening of a cavern in salt rock by dissolution, it was found that only two principal components are sufficient to explain 97% of the total variance of the parameters, in which PC1 was responsible for 79,04% and the second, PC2, for 18,04% of the data variations. Comparatively, in a study with 7 criminality characteristics of some cities in the United States, it was found that with only two components it was possible to explain 68.13% of the total variance of the characteristics [12].

JOHNSON & WICHERN [13], emphasize that it is sufficient for the retained components to represent at least 80% of the total variability of the data. Despite the first component (PC1) representing 79.04% of the total variability of the data, according to Table 7, the injection temperature parameter data has significant weight for the second component (PC2), around 70%, which justifies that this component is also considered in the study of the data set.

Table 6: Principal Components (PCs), eigenvalues (λ), and percentage of variance explained by the components

PC	Eigenvalue	% Variance
1	8.69491	79.045
2	1.98493	18.045
3	0.26294	2.3904

To understand the importance of each variable in the construction of the two components, two important relationships were shown in Table 7, the weighting coefficient, that is, the weight of each variable in the component under analysis and its correlation coefficients with the first two components main. As previously mentioned, the injection temperature variable has a significant weight in terms of the second component (PC2), not influence on the first component (PC1), the salt dissolution factor has similar comportment to injection temperature, it's happened because this coefficient depends directly on the temperature according to Eq. (3), the other variables have almost similar weight for PC1, even in PC2, radius and volume also have a small weight for the second component. As for the correlation, the injection temperature and DF are directly correlated to the y-axis, while the other variables are directly correlated to the x-axis.

Table 7: Weighting coefficients of the characteristics and their correlation coefficients with the first two principal components

Principal Component	Weighting Coefficient		Correlation	
	PC 1	PC 2	PC1	PC2
Injection Temperature	0.026337	0.6988	0.07766	0.98453
Injection Rate	0.33591	-0.053025	0.9905	-0.074706
Radius	0.32133	0.094616	0.94752	0.1333
Volume	0.32742	0.096823	0.96546	0.13641
Pump Power	0.33103	-0.052234	0.97611	-0.073591
Cumulative Energy	0.33056	-0.054977	0.97473	-0.077455
Tubing Loss	0.3369	-0.056195	0.99341	-0.079172
Produced Brine	0.33582	-0.052931	0.99022	-0.074573
Pump Pressure	0.33701	-0.048399	0.99374	-0.068188
Injection Pressure	0.33588	-0.06052	0.99042	-0.085265
Salt Dissolution Factor	0.067061	0.68762	0.19774	0.96877

Through Figure 6, a PC1 x PC2 biplot, it is possible to observe a high correlation between the variables injection rate, pump power, cumulative energy, tubing loss, produced brine, injection pressure, and pump pressure, as they are almost overlapping each other, the radius and volume variables also show a high correlation with each other. From the position in the biplot, it is noted that the injection temperature variable is isolated, next to DF, quite close to the y-axis, although they are in the same quadrant of the radius and volume, the latter doesn't seem to have a great contribution in terms of PC2.

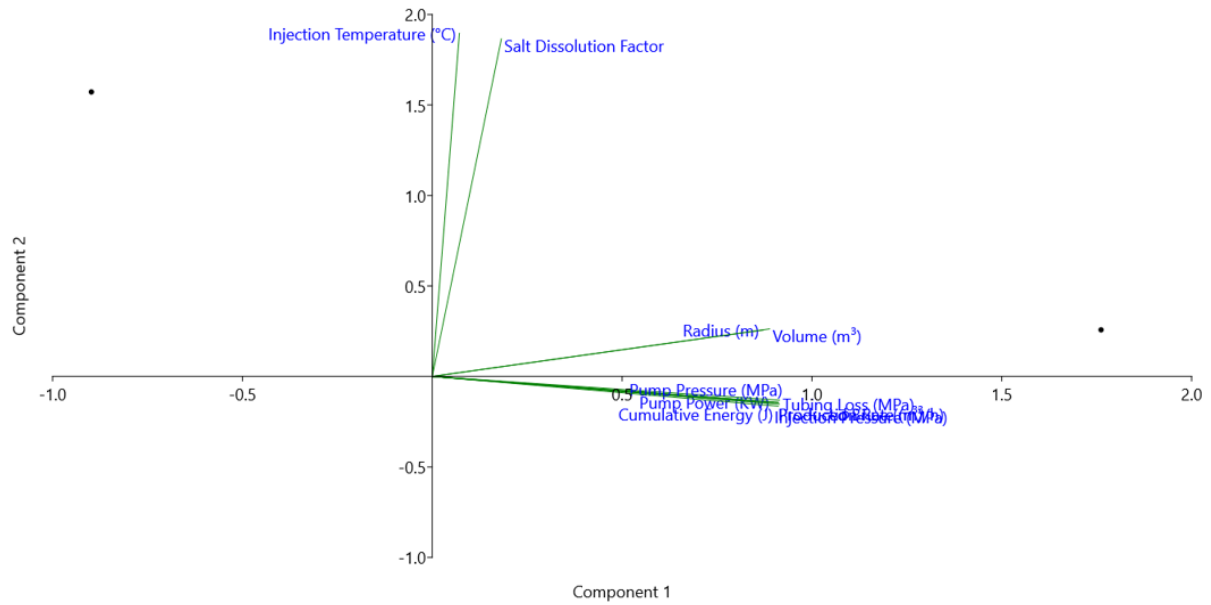


Figure 6: PC1 x PC2 Biplot

For scenario R, the results with the PCA technique were quite similar to those of scenario D, in Table 8, below, it is observed that 78,97% of the data are in terms of the first component (PC1), 17,88% in terms of the second (PC2), adding up to a total of almost 97% of variance in terms of the first two components.

Similar to what happens in scenario D, the temperature and DF in scenario R also has a significant weight in terms of the second component, around 70%, as shown in Table 9. Therefore, both components (PC1 and PC2) must be considered in the data analysis of this population.

Table 9 also shows that for PC1, the radius variable, which in scenario D had a weight and a correlation almost in the same proportion as the other variables, except injection temperature and DF, in this scenario appears to have slightly smaller participation. On the other hand, it increased its share in terms of the second component.

Table 8: Principal Components (PCs), eigenvalues (λ), and percentage of variance explained by the components

PC	Eigenvalue	% Variance
1	8.68696	78.972
2	1.96689	17.881
3	0.273911	2.4901

By the PC1 x PC2 Biplot, Figure 7, it is possible to observe that in terms of PC1, the variables injection rate, pump power, cumulative energy, tubing loss, produced brine, injection pressure, and pump pressure maintain a high correlation between them, also in the R scenario. The radius and volume variables decreased the correlation between them, compared to the D scenario. For PC2, the temperature and DF remained very close to the y axis, with the radius variable closer to the y axis as well.

Table 9: Weighting coefficients of the characteristics and their correlation coefficients with the first two principal components

Principal Component	Weighting Coefficient		Correlation	
	PC 1	PC 2	PC1	PC2
Injection Temperature	0.02688	0.69881	0.079224	0.98005
Injection Rate	0.33594	-0.054279	0.99012	-0.076124
Radius	0.31809	0.11815	0.93754	0.1657
Volume	0.32906	0.083291	0.96987	0.11681
Pump Power	0.33053	-0.059279	0.97419	-0.083137
Cumulative Energy	0.33056	-0.060614	0.97427	-0.085009
Tubing Loss	0.33682	-0.060065	0.99274	-0.084239
Produced Brine	0.33583	-0.054172	0.98983	-0.075975
Pump Pressure	0.33688	-0.054571	0.99291	-0.076534
Injection Pressure	0.33604	-0.062936	0.99044	-0.088265
Salt Dissolution Factor	0.076151	0.68349	0.22444	0.95856

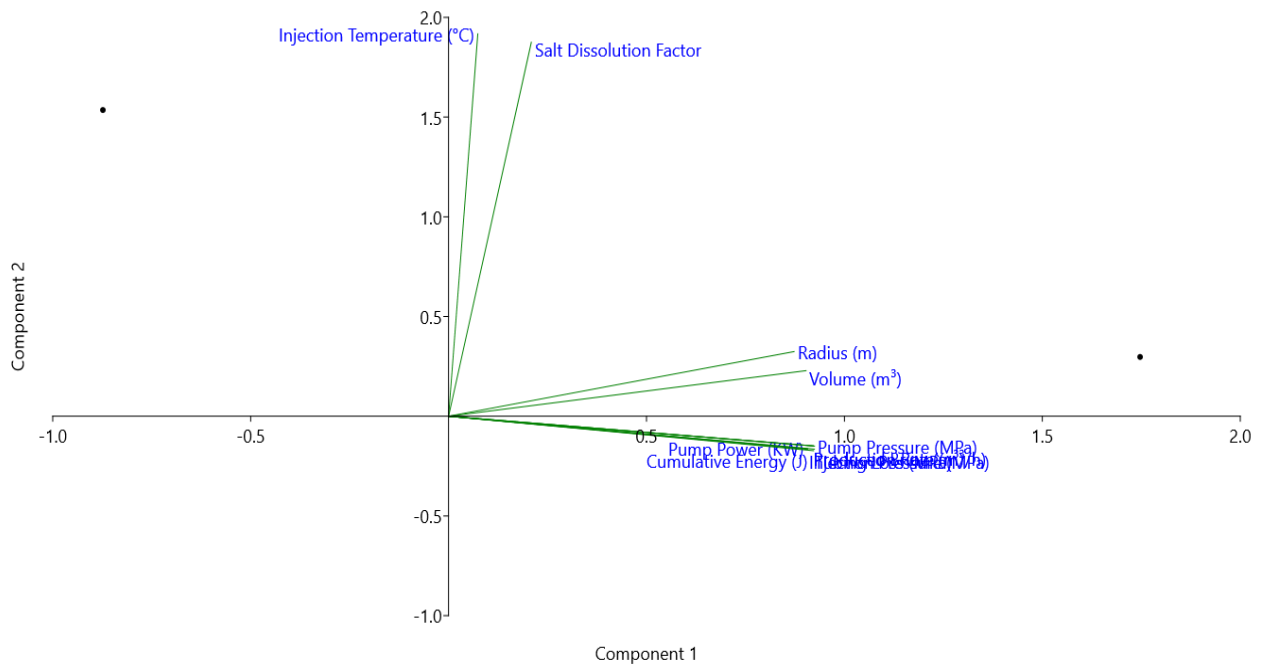


Figure 7: PC1 x PC2 Biplot

3.3 Relation DF x Injection Temperature x Injection Rate

Another important relation it's DF x Injection Temperature x Injection Rate. Considering the temperatures of 40, 60, and 80°C for the respective injection rates and salt dissolution factors, it is possible to trace a graphic

analyzing each scenario.

Figures 8 and 9 suggest low temperatures, 40°C, DF doesn't change with an increase in injection rates, it's possible to see any changes from the injection rate of 400 m³/h and injection temperature of 80°C. Similar behavior was observed in both scenarios. Therefore, one can consider in future studies, working with injection rates above 400 m³/h and injection temperatures above 60°C, since from that point, DF is really relevant.

Table 10: Data of DF, Injection Temperature, and Injection Rate to Scenario D

40°C		60°C		80°C	
Q	DF	Q	DF	Q	DF
120	1.259894	120	1.58798	120	1.670901
200	1.26017	200	1.590177	200	1.676977
360	1.260719	360	1.591269	360	1.68872
400	1.260993	400	1.592356	400	1.694402
800	1.263961	800	1.604033	800	1.750297
1200	1.268407	1200	1.622144	1200	1.824287

Table 11: Data of DF, Injection Temperature and Injection Rate to Scenario R

40°C		60°C		80°C	
Q	DF	Q	DF	Q	DF
120	1.258226	120	1.581274	120	1.630975
200	1.258506	200	1.582404	200	1.638101
360	1.258785	360	1.584649	360	1.651749
400	1.259063	400	1.585764	400	1.658297
800	1.262351	800	1.598788	800	1.726229
1200	1.267375	1200	1.618217	1200	1.809206

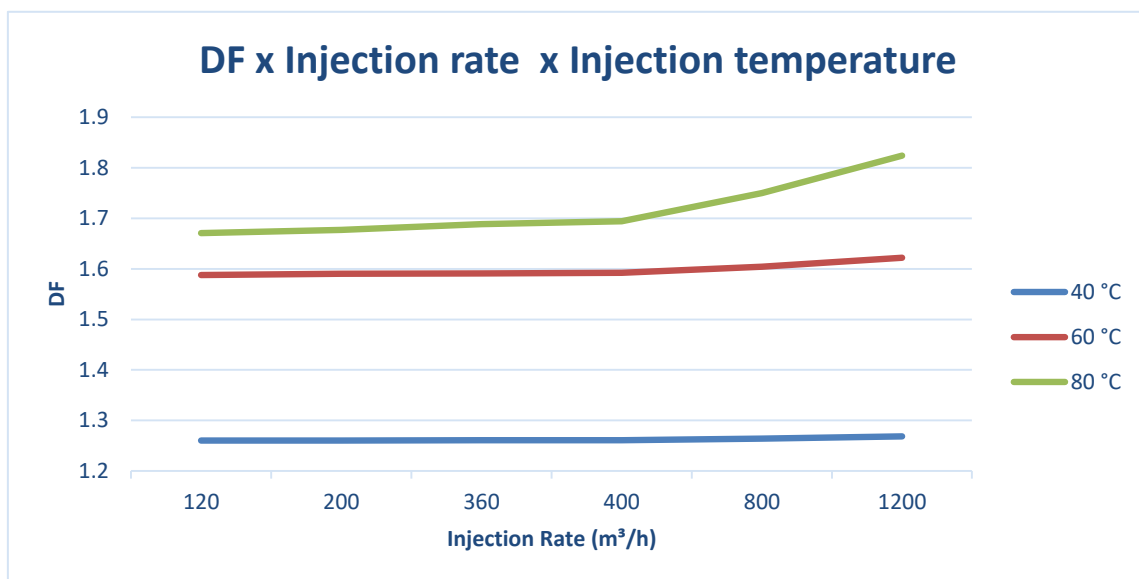


Figure 8: DF x Injection Temperature x Injection Rate to Scenario D

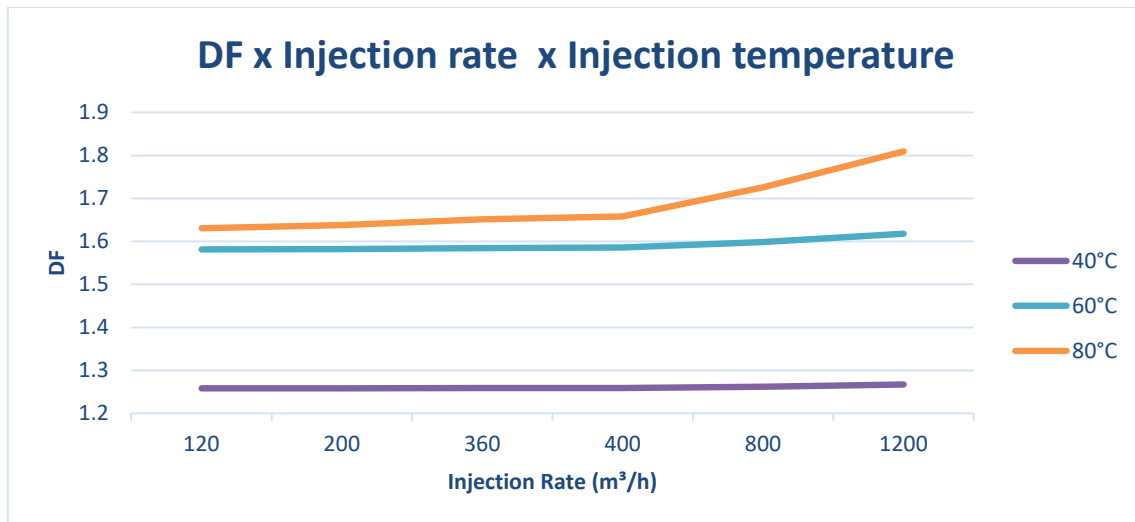


Figure 9: DF x Injection Temperature x Injection Rate to Scenario R

4. Conclusion

Taking into account the results obtained, the principal component analysis technique proved to be effective and allowed the removal of nine variables that were redundant because they were correlated with others of greater importance, that is, the 11 parameters of the numerical simulations in SalGas reduced its dimensionality to two principal components, the brine injection rate provided the most information for the x-axis and the injection temperature the largest for the y-axis, in this way, the modeling process for new scenarios can be streamlined and simplified, preserving most of the original data. Added together, the first two components represented about 97% of the total variability of the original data. As for the influence on the salt cavity opening process, in terms of PC1, the brine injection rate was the variable that most contributed to the process, being followed in the same proportion by the other variables, exception for the injection temperature and DF. These have a significant weight in terms of PC2. For the analysis of principal components, both scenarios presented almost similar results, as for the SALGAS simulations, in the proposed time of 120 days, the final geometry of the cave for the Scenario D resembled the appearance of a pear while for the Scenario R of a cone, the contour and the final volume of the cave were higher for the Scenario R, this does not imply that one scenario is more favorable than the other, since each one has its advantages and limitations. With the numerical simulations, it was also possible to conclude that the largest radius and the largest volume were found for the simulation of a higher production rate, 1200m³/h, and higher temperature, 80°C, that is, the higher the brine injection rate, the greater the radius and volume of the cave. Similar behavior is verified in relation the influence of the injection temperature, the higher the temperature, the greater the volume and radius of the cavern, although it influences to a lesser extent. Also, when analyzing the relation of DF with injection temperature and injection rate, it's possible to see that the variable temperature influences in the behavior of cavern for high temperatures and injection rates.

Acknowledgments

The authors acknowledge the Graduate Program in Civil Engineering (PPGEC) and the final support from the Brazilian research agency CAPES (Coordination for the Improvement of Higher Education Personnel), Energi

Simulation, and PETROBRAS (Brazilian Oil Company).

References

- [1] H. Mirzabozorg, K. Nazokkar, R. J. Chalaturny, and S. Nazary Moghadam. "Parametric assessment of salt cavern performance using a creep model describing dilatancy and failure". *International Journal of Rock Mechanics and Mining Sciences*, vol. 79, pp. 250-267, 2015.
- [2] S. Nazary Moghadam, H. Mirzabozorg, and A. Noorzad. "Modeling time dependent behavior of gas caverns in rock salt considering creep, dilatancy and failure". *Tunneling and Underground Space Technology*, vol. 33, pp. 171-185, 2013.
- [3] X. Yang and X. Liu. "Numerical simulation of rock salt dissolution in dynamic water". *Environmental Earth Sciences*, vol. 76, pp. 1-10, 2017.
- [4] R. W. Durie and F. W. Jessen, "Mechanism of the Dissolution of Salt in the Formation of Underground Salt Cavities". *Society of Petroleum Engineers Journal*, vol. 4, n. 2, pp. 183-190, 1964.
- [5] A. Saberian. Numerical Simulation of Development of Solution-Mined Salt Cavities. 1974.
- [6] X. Yang, X. Liu, W. Zang, Z. Lin and Q. Wang. "A Study of Analytical Solution for the Special Dissolution Rate Model of Rock Salt". *Advances in Materials Science and Engineering*, vol. 2017, pp. 1-8, 2017.
- [7] D. F. FERREIRA. *Estatística Multivariada*. 2.ed. Lavras: UFLA, 2011, vol.1, pp. 1-676.
- [8] J. Alonso-Gutierrez et al., "Principal Component Analysis of Proteomics (PCAP) as A Tool to Direct Metabolic Engineering". *Metabolic Engineering*, vol. 28, pp. 123 – 133, 2015.
- [9] J. K. Warren. *Evaporites: Sediments, Resources and Hydrocarbons*. Berlin: Springer, 2006, pp. 1-1036.
- [10] T. Eyerman, *SALGAS and SalGas for Windows User's Manual*. pp. 1-53, 2008.
- [11] A. Saberian. *SALGAS User's Manual, Volume 1 and 2*. Solution Mining Research Institute, Clarks Summit, PA, 1984.
- [12] K. Hongyu, V. L. M. Sandanielo and G. J. Junior. "Principal Component Analysis: theory, interpretations and applications". *E&S - Engineering and Science*, vol.1, n. 5, pp. 83-90, 2015.
- [13] R. A. Johnson, D. W. Wichern. *Applied multivariate statistical analysis*. Madison: Prentice Hall International, pp. 1-816, 1998.